CERN-ACC-2020-0015

Oliver.Bruning@cern.ch

Report

LHC Full Energy Exploitation Study: Upgrade for Operation Beyond Ultimate Energy of 7.5TeV

Andrea Apollonio, Susana Izquierdo Bermudez, Luca Bottura, Krzysztof Brodzinski, Oliver Brüning, Serge Claudet, Dimitri Delikaris, Riccardo De Maria, Massimo Giovannozzi, Brennan Goddard, Anton Lechner, Felix Rodriguez Mateos, Thys Risselada, Frédéric Savary, Andrzej Siemko, Ezio Todesco, Rogelio Tomas, Davide Tommasini, Rob van Weelderen, Daniel Wollmann, Markus Zerlauth

CERN, Geneva, Switzerland

Keywords: LHC, HL-LHC, and energy upgrade beyond ultimate beam energy

Abstract

This report looks at the feasibility and limitations of upgrading the HL-LHC for operation beyond the ultimate beam energy of 7.5 TeV by means of replacing a fraction of the nominal LHC dipole magnets with 11 T Nb_3Sn magnets.

Geneva, Switzerland
September, 2020

Contents

1 Introduction

This paper is the third and last report of a series on the full-energy exploitation of the LHC. The first report [1] addressed the question of the feasibility, required steps, and efficiency of operating the LHC at its nominal beam energy of 7 TeV and a magnetic dipole field of 8.3 T (an increase of 0.5 TeV with respect to the operation beam energy in Run 2). The second report [2] addressed the question of feasibility, required steps, upgrades, and potential machine efficiency for operating the LHC machine at its 'ultimate' beam energy of 7.5 TeV, corresponding to a dipole field of 8.93 T. This third report evaluates the possibility of increasing the energy in the LHC beyond the ultimate beam energy by replacing approximately one third of the LHC Nb-Ti dipole magnets with 11 T Nb_3Sn magnets that have already been developed in the framework of the HL-LHC upgrade. Assuming that all remaining nominal Nb-Ti magnets are operated at ultimate current, such an upgrade could, on paper, offer at best a beam energy of up to 8.08 TeV – e.g. an increase of 7.7% with respect to the ultimate beam energy. This will be the basis for the following study. If one assumes operation of the nominal Nb-Ti magnets at lower currents, the potential gain in beam energy will be even less.

The task of this report is to evaluate if such an upgrade is feasible, given the LHC infrastructure and schedule, or if it is excluded on principle grounds or implies significant additional hardware upgrades for the LHC accelerator complex beyond the installation of the 11 T dipole magnets. This upgrade can certainly only be foreseen at the end of the HL-LHC era and the evaluation should therefore be done under the assumption that the full HL-LHC upgrade has already been implemented and commissioned.

2 Summary of findings of the first and second report for operation at nominal and ultimate beam energy

The first report addressed the open issues and performance reach of the LHC for operation at the nominal beam energy of 7 TeV [1]. The main points were to estimate the time required for training the magnet system for operation at 7 TeV, to identify potential bottlenecks in the technical infrastructure, to recommend technical upgrades prior to the operation at 7 TeV, and to estimate the potential performance reach of the machine at 7 TeV beam energy. The main outcome of the first report was the confirmation of risks associated with short to grounds that can develop in the LHC dipole magnet diode boxes during a quench and the occurrence of multiple quenches at higher magnet fields.

In agreement with the LHC experiments, the discussions ensuing the preparation of the first report led to the decision to keep the beam energy at 6.5 TeV during the full LHC Run 2 period and to plan for operation at 7 TeV only after LS2, i.e. after the repair of critical magnet non-conformities and the consolidation of the diode box insulation.

While not finding intrinsic limitations in the LHC machine that would prevent operation at ultimate beam energy, the second report [2] highlighted that the compatibility of the complete HL-LHC magnet system for operation at ultimate beam energy still needs to be demonstrated and identified systems in the nominal LHC that require upgrades, e.g. Q6 in Point 6 most certainly requires an upgrade of the cryogenic system from 4.5K to 1.9K and the LHC Beam Dump System and the heat load due to electron cloud-related phenomena. The second report also identified circuits that require special attention and training efforts for reaching the ultimate beam energy of 7.5 TeV (e.g. the superconducting D3 separation dipole magnets in IR4).

Furthermore, the second report [2] estimated the dedicated training time for the magnet circuits to reach ultimate field at ca. 6-12 months. If not resolved and mitigated by other means, the larger-than-

expected heat load due to electron cloud effects in the LHC Run 2 operation[1] will impose a beam intensity limitation at higher beam energy. The increased heating from synchrotron radiation at higher beam energies adds to the cooling requirements at ultimate beam energy [increase of up to 7%] and therefore adds to the potential intensity limitations for operation at ultimate beam energy.

The reduction of the quench margins in the magnet system at higher than nominal beam energies will imply more frequent beam aborts and, together with the longer cycle and recovery time for operation at higher beam energies, implies a loss of up to 30% in integrated luminosity for operation at 'ultimate' beam energy when comparing the performance reach of the HL-LHC to that at nominal beam energy with conservative fault scenarios.

3 Key Systems

In this section we address and highlight critical aspects of key LHC systems that arise in addition to the points mentioned already in [2] for operation at 'ultimate' beam energies.

3.1 Cryogenics

In addition to a further increase of the heat load due to synchrotron radiation (ca. 35% increase due to the higher beam energy), the operation with a substantial assembly of 11 T dipole magnets will have to cope with the additional heat load due to the magnetization cycle of the 11 T magnets and its implication to the cryogenic system. Each sector of about 3.3 km has available a maximum cooling power of 0.8 W/m when averaged over its full length. Given a static load of about 0.5 W/m, a residual cooling power of about 0.3 W/m is available to deal with sector-wide transients. In the current LHC, Nb-Ti dipole current ramp dissipation is about 0.1 W/m which, given the 0.3 W/m available residual cooling power, has an almost invisible effect on the average magnet temperatures. This is minimized even further by the temperature buffering effect of the ~25 ℓ/m helium coolant contained in the magnets' cold masses. In contrast, the Nb_3Sn-based 11 T dipoles contribute an estimated current ramp dissipation of ~ 5.3 W/m each (~ 2207 J/m/aperture × 2 apertures in 839 s), i.e. ~79 W per 11 T dipole. Averaged over the full sector, it raises the transient power that would need to be extracted during current ramp cycles to 1.7 W/m, without even including the increase in synchrotron radiation. This is more than 5 times the 0.3 W/m available residual cooling power. As a consequence, the magnet temperatures are estimated to rise by ~70 mK for each current ramp (up or down). Estimated re-cooling rates are in the order of 40 mK/hour – 50 mK/hour. This will impact the possible modes of current cycling and increase the overall machine turnaround time. Starting from 1.90 K with subsequent current ramps one would soon exceed the lambda temperature of 2.17 K at which cooling will break down, unless one accepts 1 hour – 1.5 hour of re-cooling times in between. One would have to operate all cooling loops and refrigerators at their maximum, without any contingency. Any minor degradation in performance of the cooling system or minor increase in heat load will jeopardise the powering of the accelerator.

The second report on the Full Energy Exploitation of the LHC concluded already, that the heat load in the arc cells is dominated by the electron-cloud effect and that operation at the ultimate beam energy of 7.5 TeV will require a Secondary Emission Yield well below 1.35 or special filling patterns that reduce the electron-cloud related heat load (and luminosity reach) in order to stay within the heat capacity of 160 W per arc half-cell. This limitation, due to the existing heat capacity in the HL-LHC arc cells, will only be worse for operation with a beam energy beyond ultimate[1].

[1] The option of replacing a fraction of the dipole magnets, the topic of this 3rd report, also represents an opportunity for upgrading the beam vacuum system for electron-cloud effects [e.g. aC coating] and therefore mitigating the above limitation – albeit at additional cost.

3.2 Magnet Construction and Integration

3.2.1 Magnet Production Options and Timescales

The hypothesis that we make here is that the construction of the 11 T magnets (referred to as MBH) will be based on the extrapolation of the technology adopted for the HL-LHC magnets. In particular, the coil cross section and structure (collars and split yoke in a welded steel shell) will stay essentially the same, fitting in a cold mass and cryo-magnet of diameter identical to that of an LHC Nb-Ti dipole (referred to as MB). The strand and cable will also be the same as procured for the HL-LHC MBH magnets. Nonetheless, a number of modifications and developments will be necessary to fit in a scheme like the one conceived, with every mid-cell dipole MB substituted by an MBH.
The first and most obvious change is the unit length of the cold mass, that should be the nominal 15.16 m of an MB cold mass (for compatibility reasons), while the standard HL-LHC MBH has a cold mass length of 6.252 m. We can envisage two scenarios, namely:

- Build the new MBH cold mass as the assembly of three HL-LHC MBH magnets of approximately 5 m length, i.e. similar to what is being produced for HL-LHC. Each magnet could be built straight (as for the HL-LHC MBH), and three of them assembled in a cold mass that would align the magnets along the desired sagitta. The advantage of this solution would be to use proven technology and existing tooling design for the magnet construction. In addition, the prototyping phase could be short, as by the time of construction the HL-LHC MBH program would have demonstrated the feasibility and performance. The drawback of this solution would be the loss of integral dipole field in the space between magnets, which would be of the order of 0.5 m per interconnect. Based on a total magnetic length of 14.3 m, this would correspond to a reduction of the theoretical integral dipole field by 7 % and thus a reduction of the potential beam energy reach from 8.08 TeV to 7.85 TeV.
- Build the new MBH from single coils of approximately 14.5 m length (as for the present MB), either straight or curved, see later, and assembled in a single collared coil per aperture. This solution has the advantage of achieving maximum integral dipole field. The main drawback is that this would be an unprecedented realization, twice as long as the longest Nb_3Sn coils built for HL-LHC, and will hence require new design features, e.g. to cope with dimensional change during manufacturing, new tooling and production infrastructure (e.g. heat treatment oven and impregnation tank). Though the changes with respect to the HL-LHC Nb_3Sn magnets are not fundamental, they will require thorough validation of the design extrapolation, and suitable prototyping, as discussed later.

The above scenarios translate into three options for the manufacturing of the new MBH cold masses, namely three straight magnets, one straight long magnet, or one curved long magnet. An evaluation of the magnet aperture is provided later. Depending on the selected cold mass configuration, the timescale of magnet construction will be different, mostly affected by required development and prototyping in the case of long coils.

For the case of a cold mass built using short straight magnets, provided funding and personnel resources are available, the required development would be modest and limited to the assembly of magnets in a single cold mass cylinder of suitable final geometry. We estimate that prototypes (typically two units) of one such magnet could be produced at CERN over a relatively short time scale (ca. 2 years). Series production on the other hand would require a significant technology transfer to industry, as a production of this scale (of the order of 500 cold masses) cannot be envisaged on CERN premises. Given that the magnet production will be in essence the same as for the HL-LHC MBH, it is expected that magnet and tooling design and procedures can be directly transferred to industry. Industry would then proceed to magnet and tooling review and design (ca. 1 year), specification and procurement (ca. 1 year), followed by an industry prototyping phase (ca. 1 year), and series production (ca. 3 years) for a

total of ca. 8 years. We assume, that superconductor procurement and cable production will run in parallel to the magnet development, prototyping and production. The lead time required for superconducting cable production is 1.5 years, in advance of coil production. The lead time required for cryostating and testing will trail by about one year after the end of the construction of the last magnet. These estimates lead then to a **10-year timescale for the delivery for installation**. This time scale is relatively optimistic and assumes only minimal deviations from the present technology.

In case of magnets built with long coils, straight or curved, the present design of the HL-LHC MBH cannot be simply adjusted, and will require extensive redesign and prototyping. Making the hypothesis that the HL-LHC MBH cross section is kept "as is", and focusing only on the adjustments required for longer length, we estimate that prototypes of this type (order of five units) could be produced at CERN over a time scale of 5 years. A longer time is required with respect to the previous option because of the design modifications, and the fact that new general tooling will need to be procured (heat treatment oven, impregnation chamber). It should be finally recognized that this option has higher technological risk. As to the transfer of technology to industry, the initial phase may also be longer than in the previous case, as here procedures and manufacturing plans will not completely profit from the validation provided by the HL-LHC MBH. Adding the time required to initiate superconducting cable production and the time to finish cryo-magnet testing, **we can envisage delivery of long MBH for installation over a timescale significantly longer than 10-years.**

Assuming that a decision could be taken at the earliest in 2020, the option of long MBH dipole magnets could not become available during the estimated HL-LHC operation period (the HL-LHC machine is expected to stop operation between 2037 and 2039 when the accumulated radiation dose will require the replacement of several critical magnet components). Even the solution based on three short MBH magnets within one cryostat could, at the earliest, be envisaged for the last HL-LHC running period with a potential installation in the Long Shutdown 5 in between 2034 and 2035, leaving only one running period for the exploitation of this upgrade with a potential beam energy of up to 8.08 TeV (if 1/3rd of all MB dipole magnets can be replaced by 11 T dipoles of equal length). One should note here that a scenario of replacing all LHC magnets will not increase dramatically the above estimates as the main driver for the timescale is the preparation and prototype development. The actual series magnet production could probably be upscaled by having more production lines in parallel.

To estimate the magnet cost of the options discussed above we take as baseline the cost of the production of the HL-LHC MBH. This can be decomposed in a R&D cost (as appropriate, including prototyping), tooling cost (general and contact), material and personnel cost for production. A cost estimate is reported in the table below in MCHF, for the three options considered. In all cases considered, the total magnet cost alone amounts to slightly more than 3 BCHF.

Table 1: Cost estimate for the different 11 T magnet configurations in MCHF

	3 straight magnets	one straight magnet	one curved magnet
R&D and prototyping	20	40	45
Tooling	100	75	75
Material	1700	1720	1720
Personnel	1400	1200	1200
Total	3220	3035	3040

It should be highlighted, that the above estimates do not include costs of other upgrades like the circuit powering and QPS system as well as the removal, transport and installation process etc. and assume that the quadrupole circuits can remain in their existing configuration.

3.2.2 Arc Aperture

In the following aperture analysis, we look at the case of a long Nb_3Sn magnet design.

The radius of curvature in a uniform dipole is given by:

$$[1] \qquad \frac{1}{R} = \frac{q\,B[T]}{p}$$

For a 11 T dipole magnet and a 7 TeV proton beam one obtains a radius of $R_{11\,T}$ = 2121 m. For a magnetic field of 8.33 T one obtains a radius of R_{8T} = 2804 m. The deflection angle is then approximately given by the length of the magnet divided by the radius of curvature and one obtains for 14.3 m long dipole magnets $\alpha_{11\,T}$ = 6.74 mrad and α_{8T} = 5.1 mrad for the 11 T and 8.33 T dipole magnets, respectively. The sagitta of the trajectory in the magnetic field can be approximated by

$$[2] \qquad h = R - \frac{1}{2}\sqrt{4R^2 - s^2}$$

with s, the arc length, given by

$$[3] \qquad s = 2R\,\sin\frac{\alpha}{2}$$

For small deflection angles one obtains thus for the sagitta:

$$[4] \qquad h \approx R\,\frac{\alpha^2}{8}$$

For a field of 11 T and a magnet length of 14.3 m one obtains thus a sagitta of approximately h = 1 2mm and replacing a curved LHC dipole magnet with a straight 11 T dipole magnet will cost approximately ±6 mm horizontal aperture along the magnet. The LHC dipole magnets have an inner coil diameter of 56 mm and an inner cold bore diameter of 50 mm at room temperature. The 11 T dipole magnets for the dispersion suppressor collimators have a slightly larger inner coil diameter (60 mm inner coil diameter), but are equipped with the same cold bore as the nominal LHC dipole magnets. Replacing the standard LHC cold bore tube with a larger tube would increase the magnet aperture by potentially up to 4 mm in diameter, provided a new type of beam screen is designed, produced, and installed in the 11 T and can be connected to the existing, nominal LHC MB beam screens. Of possible relevance could be issues related to the connection of the cooling capillaries and local losses and impedance effects due to aperture transitions. However, this is still a smaller gain than the 12mm loss due to the trajectory sagitta in a straight 11 T dipole magnet. Therefore, even with an increased cold bore tube, the use of straight 11 T dipole magnets will result in a net loss of 8mm in the cold bore diameter.

Table 2 shows the results of the aperture computations based on the standard assumptions used for HL-LHC [3], [4], together with the values of the aperture loss in nominal and 11 T dipoles for two possible configurations [5], the LHC Nb-Ti magnets either running at nominal or at ultimate energy plus 1/3rd of the magnets replaced by 11 T magnets, providing different values of the beam energy. The optics used is the HL-LHC V1.4 [6]. The aperture loss for the 11 T dipole is the total loss obtained by the estimate of the sagitta reduced by the potential aperture gain due to the installation of a special beam screen of increased aperture. For the case of the nominal dipoles the aperture loss is estimated by taking the difference between the nominal LHC value of the sagitta, i.e. 9.14 mm, and the computed value for the two beam energies.

Table 2: Summary of the aperture estimate for the two possible configurations with one third of the main dipoles replaced by 11 T dipoles.

Beam Energy (TeV)	Aperture loss		Aperture estimate	
	11 T dipole (mm)	Nominal dipole (mm)	Round (σ)	Flat (σ)
7.75	7	0.8	19	18
8.08	4.3	2.3	21	19

Note that for the arcs the target aperture value is between 18 σ and 20 σ and that for the nominal HL-LHC optics V1.4 the typical aperture in the arcs is between 22 σ and 19 σ for round and flat variants, respectively. For the option at 7.75 TeV a net aperture loss of 3 σ is observed for the round optics, but it is still just sufficient. However, the additional 1 σ reduction for flat optics brings the aperture estimate at the lower bound of the interval of acceptable aperture. For the sake of accuracy, the aperture bottlenecks occur at the location of the dispersion correction bumps in the arcs 4-5 and 5-6. At 8.08 TeV the situation in terms of aperture improves due to the higher beam energy and rigidity and essentially no limit is observed.

Replacing every mid-half-cell dipole magnet of the nominal arc cell with an 11 T dipole magnet will change furthermore the particle trajectory along the LHC cells. In order to compensate for this trajectory change and to assure that the start and end points of the cell trajectory coincide with those of the nominal LHC cells, the magnets within the cell need to be transversely repositioned. The total deflection angle along the modified LHC cell is assumed to be constant (reduced deflection angle in the 8.33 T magnets due to the increase in beam energy). The transverse shift of the magnets is comparable in magnitude to the trajectory sagitta within the magnet and opposite in sign. Figure 1 shows the survey position of the magnets in the LHC cell. The top figure shows the horizontal survey coordinates as a function of the 's' coordinate, i.e. position along the circumference, for the nominal LHC cell and a layout where every mid-half-cell magnet is replaced by a 11 T magnet. The lower figure shows the difference in the transverse survey positions between the two cases. The difference data shows that the position of the 11 T dipole magnets needs to be shifted by approximately 7mm with respect to the nominal 8.33 T dipole positions in order to keep the trajectory positions at the extremities of the cell equal to that of the nominal LHC cells. The potential impact of this shift on the interconnectability of the dipole magnets still needs to be looked at in more detail. This required shift of 7 mm approximately compensates the required shift for the trajectory sagitta inside the 11 T magnets but will reduce the usable aperture at the magnet extremities and might imply adaptations to the magnet interconnections.

The LHC features 23 regular cells for each of the eight arcs. Replacing every mid-half-cell dipole magnet with new 11 T magnets requires therefore for the LHC arcs a total of **2×23×8 = 368** new, 14.3-meter-long, 11 T dipole magnets, without considering those located in the dispersion suppressors. Figure 2 shows the resulting survey shift with respect to the survey data of the nominal LHC over the whole length of the machine. One observes a maximum shift of ca. 8.5 mm along the arcs of the LHC.

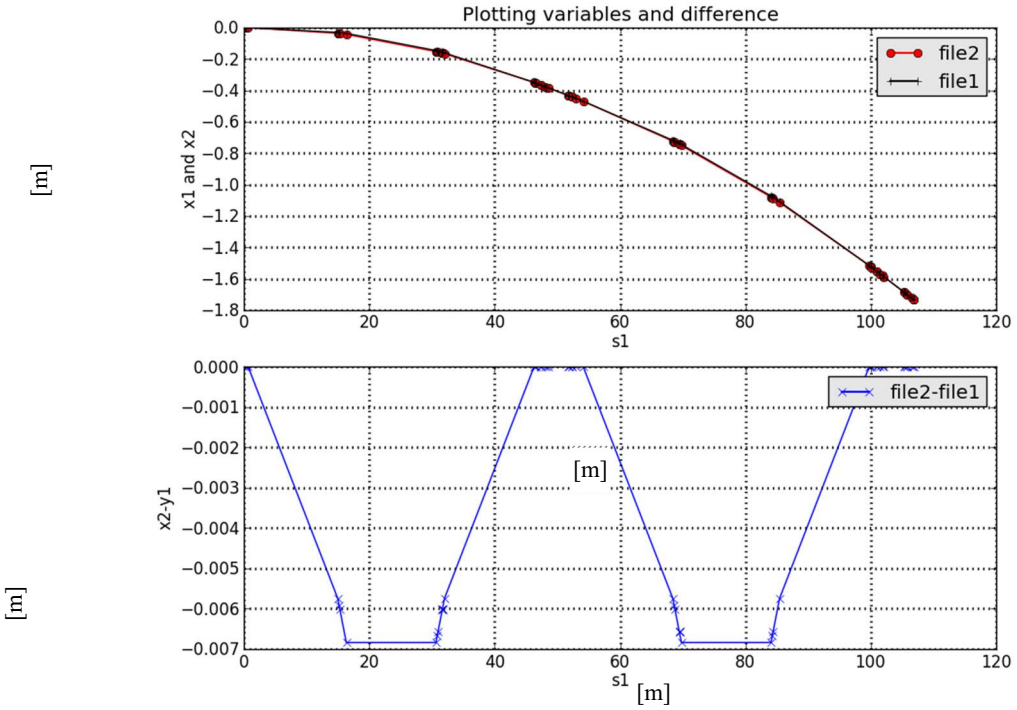

Figure 1: Survey position of the magnets in the LHC cell. The top figure shows the survey coordinates in the transverse plane for the nominal LHC cell and a layout where every 3rd dipole magnet is replaced by a 11 T magnet. The lower figure shows the difference in the transverse position between the two cases.

3.2.3 Dispersion Suppressor Layout

The cell structure of the dispersion suppressor section is more complicated than that of the nominal LHC arc cell. It serves two basic functions: a) to reduce the arc dispersion and b) guide the beam trajectory along the geometry of the LEP tunnel. The dispersion suppression is achieved via a missing-dipole concept. The LEP dispersion suppressor was made of 3.5 LEP cells with a 90-degree phase advance and missing dipole magnets. The layout was optimized for the LEP dispersion suppression. With the 2.5-times longer LHC cells, the LHC dispersion suppressor can only host 2 cells with missing dipole magnets, i.e. 2 instead of 3 dipole magnets per half-cell. The LHC dispersion suppressor is therefore slightly incomplete and the dispersion suppression must be accompanied in the LHC with individual quadrupole powering in the dispersion suppressor section. Just replacing every 3rd dipole magnet of the LHC cell with a 11 T dipole magnet, as done in the arc cells, will therefore not preserve the tunnel geometry as in the dispersion suppressor the number of main dipoles is not a multiple of three and hence the same approach as in the regular cell cannot be applied. The LHC dispersion suppressor section therefore either requires a replacement of all 8.33 T dipole magnets by stronger magnets, i.e. requiring **2×8×8 = 128** additional new dipole magnets on top of the 368 new 11 T magnets required for the LHC arc cells and / or a completely revised dispersion suppressor layout with more individually-powered quadrupole magnets.

An upgrade of the dispersion suppressors will require a special powering of the dipoles, which requires either a different power converter with respect to that of the arc dipoles or by means of trim power converter in addition to the series powering with the arc dipoles. Some studies have been carried out to assess what could be possible layouts for the new dispersion suppressors under different assumptions concerning the number of main dipoles to be replaced. Some layouts are shown in Figure 3, where the radial offset with the respect to the current layout of the dispersion suppressor is shown.

The layouts are made of three families of dipoles, namely nominal dipoles powered at 9 T, Nb_3Sn dipoles powered at 11 T, and Nb_3Sn dipoles powered at lower field. This implies that while the 9 T and 11 T dipoles can be powered in series with the arc dipoles the other dipoles should be powered independently or in series with the arc dipoles, but with a trim power converter. The scheme shown on the right requires a smaller number of additional 11 T dipoles than that on the left. However, the two differ in terms of ring geometry, although the differences seems to be acceptable. In Table 3 a summary of the characteristics of some configurations analysed is reported. It clearly shows that the use of only main dipoles or only 11 T dipoles it is not possible to match the tunnel geometry. This can be achieved only by adding a number of Nb_3Sn dipoles with special powering to achieve a given field level.

LHC dispersion suppressor in IR7 features for the HL-LHC in addition special dispersion suppressor collimators that are implemented with the help of 5-meter-long 11 T dipole magnets. Indeed two 5-meter-long 11 T dipole magnets replace one nominal LHC 8.33 T magnet, leaving sufficient space for the installation of a collimator. Upgrading the LHC dispersion suppressor in IR7 with stronger dipole magnets therefore either requires also the replacement of the existing 11 T magnets with stronger magnets or a complete reshuffling of the dispersion suppressor layout in order to integrate the collimators. The first option requires the development of new, even stronger dipole magnets and the latter implies significant installation work, comparable to the intervention work done after the 2008 incident. Figure 2 shows the resulting survey data for the whole LHC machine assuming that the layout of the dispersion suppressor sections remains unchanged with respect to that of the nominal LHC.

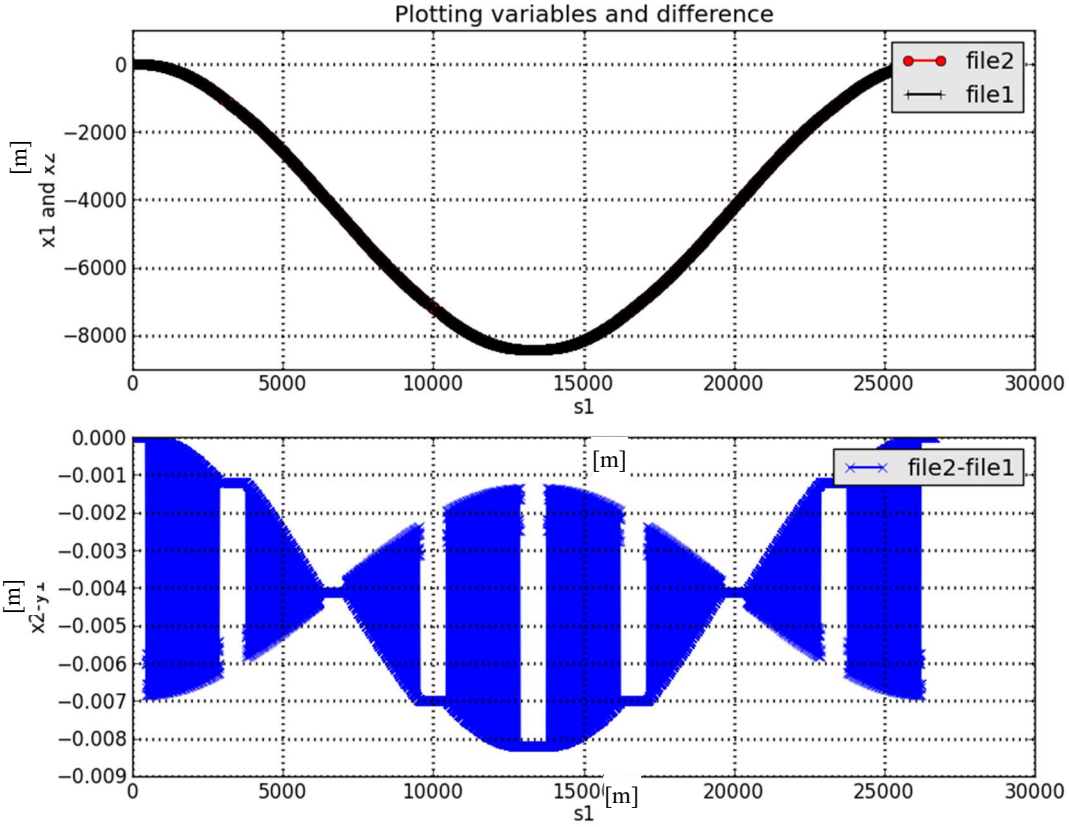

Figure 2: Resulting survey data for the whole LHC machine ignoring the DS layout challenge and assuming an identical DS layout as in the current LHC. The top figure shows the survey coordinates in the transverse plane for the nominal LHC cell and a layout where every 3rd dipole magnet is replaced by a 11 T magnet. The lower figure shows the difference in the transverse position between the two cases.

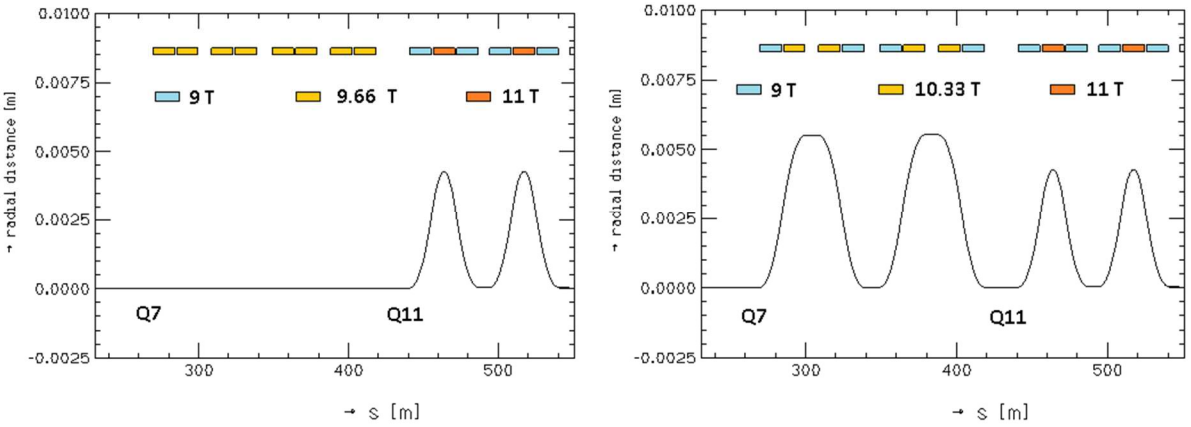

Figure 3: Possible layouts of the new dispersion suppressors using various families of dipoles. Those indicated by 9 T and 11 T can be in series with the arc dipoles, while those featuring different field will be made of 11 T dipoles with different powering.

Table 3: Summary of the characteristics of some configurations analysed is reported.

DS configuration	DS deflection (mrad)	Peak-to-peak survey offset [m]	
		DS(m)	Arc
Present LHC	40.80	0.000	0.000
Only 9 T dipoles	38.26	0.246	1.826
With 2 dipoles at 11 T	40.17	0.026	0.411
With 3 dipoles at 11 T	41.11	0.008	0.197
With 3 dipoles at 10.78T	40.80	0.031	0.004
With 4 dipoles at 10.33T	40.80	0.006	0.004
With 8 dipoles at 9.67T	40.80	0.000	0.004

3.2.4 Insertion Region Layout

The two LHC proton beams follow different trajectories along the LHC arcs, the dispersion suppressors and most of the matching sections of the LHC. Dedicated separation-recombination dipole magnets bring the two beams onto common trajectories in the long straight sections that feature beam collisions and experiments and special dogleg dipole magnets increase the separation of the two proton beams in the service insertions IR3 and IR7 that host the collimator systems and in IR4 that hosts the RF system and the beam diagnostics. All the dogleg dipole magnets are 2-in-1 magnets and half of the separation-recombination dipole magnets are 2-in-1 magnets. The other half of the Separation-Recombination dipole magnets has single apertures. The cleaning insertions IR3 and IR7 feature normal conducting dogleg dipole magnets. The possibility of these magnets to go beyond ultimate energy should be assess in detail, also considering the possible impact of saturation effects. The same should be done for the warm quadrupole magnets in both insertions.

Increasing the beam energy in the LHC through the use of 11 T dipole magnets in the arc, therefore also requires upgrades of the existing superconducting separation-recombination and dogleg dipole magnets. In total this requires the development of 4 new, 2-in-1 superconducting dogleg magnets for IR4 and 8 2-in-1 and 8 single aperture separation-recombination dipole magnets in the experimental insertions, implying in total the development of **32 new superconducting magnets with 64 coils and including a required R&D and short model magnet development program**.

3.2.5 Magnetization heat load

The total heat losses for an 11 T magnet during a full cycle from nominal field down to injection and up to nominal field again, are 8 kJ/m at 1.9 K for the two apertures. The loss mainly comes from the magnetization of the superconductor and it is independent of the ramp rate. The induced heat deposition needs to be considered when looking at the operational margins for the cryogenic system (see section 3.1). The total heat deposition depends on the cable and wire design and can be optimized w.r.t. that of the existing MBH design that has been optimized under other constraints and boundary assumptions, e.g. only a small number of installed magnets. Figure 4 shows the hysteresis loss profile per magnet aperture for the standard LHC cycle to nominal current.

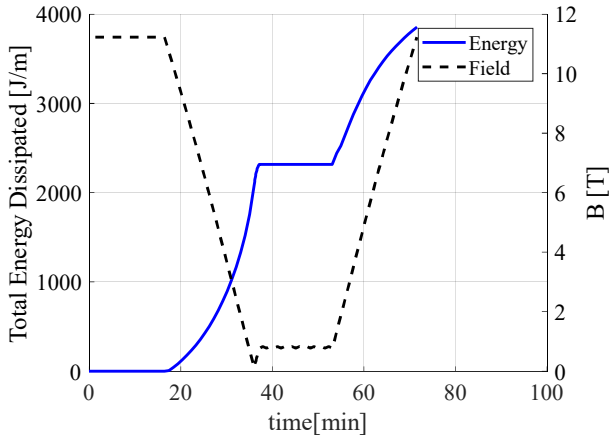

Figure 4: Hysteresis loss profile per magnet aperture for the standard LHC cycle to nominal current.

3.2.6 Field quality

The different contribution of the field errors in the 11 T magnet are given in Table 4 [7]. The values of the multipoles are given in units of 10^{-4} relative to the main field (e.g. dipole field), at a reference radius of 17 mm. The b_n coefficients refer to the normal field errors and the a_n components to the skew errors. For example, b_2 refers to a normal quadrupole field, b_3 to a normal sextupole and a_2 to a skew quadrupole. It is common to distinguish systematic, uncertainty and multipole errors. The uncertainty represents the systematic difference between production lines and the random component corresponds to the variation from magnet to magnet. Uncertainty and random components are assumed to have the same amplitude, and are estimated for a 60 μm random error in the block positioning. Based on the experience of the 11 T short and long magnet models, the random errors are multiplied by a factor two for the allowed harmonics at collision energy and by a factor four at injection energy.

Table 4: Normal and skew multipole errors in the 11 T dipole at injection and top energy (7.5 TeV) [7].

	DS-11 T Dipole field quality version 1 February 2019 R_{ref}=17 mm (7.5 TeV)								
	Systematic					Uncertainty		Random	
Normal	Geometric	Saturation	Persistent	Injection	High Field	Injection	High Field	Injection	High Field
1						20	20	20	20
2	0.000	-17.836	0.000	0.000	-17.836	1.705	1.705	1.7045	1.705
3	7.500	-0.367	-8.800	-1.300	7.133	4.315	2.158	4.3152	2.158
4	0.000	-0.929	0.000	0.000	-0.929	0.623	0.623	0.6229	0.623
5	-0.014	0.428	2.400	2.386	0.414	1.396	0.698	1.3960	0.698
6	0.000	-0.021	0.000	0.000	-0.021	0.175	0.175	0.1746	0.175
7	-0.093	0.060	0.400	0.307	-0.033	0.407	0.203	0.4068	0.203
8	0.000	0.000	0.000	0.000	0.000	0.055	0.055	0.0551	0.055
9	0.912	0.031	0.400	1.312	0.943	0.114	0.057	0.1144	0.057
10	0.000	0.002	0.000	0.000	0.002	0.013	0.013	0.0131	0.013
11	0.450	0.000	0.000	0.450	0.450	0.026	0.013	0.0260	0.013
12	0.000	0.000	0.000	0.000	0.000	0.003	0.003	0.003	0.003
13	-0.115	-0.006	0.000	-0.115	-0.121	0.000	0.000	0.000	0.000
14	0.000	0.000	0.000	0.000	0.000	0.000	0.000	0.000	0.000
15	-0.032	-0.002	0.000	-0.032	-0.034	0.000	0.000	0.000	0.000
Skew									
2	0.000	-0.260	0.000	0.000	-0.260	1.820	1.820	1.660	1.820
3	-0.130	-0.930	0.000	-0.130	-1.060	1.180	1.180	1.000	1.180
4	0.000	-0.112	0.000	0.000	-0.112	0.673	0.673	0.640	0.673
5	0.080	-0.012	0.000	0.080	0.068	0.389	0.389	0.380	0.389
6	0.000	0.000	0.000	0.000	0.000	0.202	0.202	0.200	0.202
7	0.030	0.000	0.000	0.030	0.030	0.103	0.103	0.090	0.103
8	0.000	0.000	0.000	0.000	0.000	0.051	0.051	0.050	0.051
9	0.000	0.000	0.000	0.000	0.000	0.024	0.024	0.030	0.024
10	0.000	0.000	0.000	0.000	0.000	0.013	0.013	0.020	0.013
11	0.000	0.000	0.000	0.000	0.000	0.007	0.007	0.010	0.007
12	0.000	0.000	0.000	0.000	0.000	0.000	0.000	0.000	0.003
13	0.000	0.000	0.000	0.000	0.000	0.000	0.000	0.000	0.000
14	0.000	0.000	0.000	0.000	0.000	0.000	0.000	0.000	0.000
15	0.000	0.000	0.000	0.000	0.000	0.000	0.000	0.000	0.000

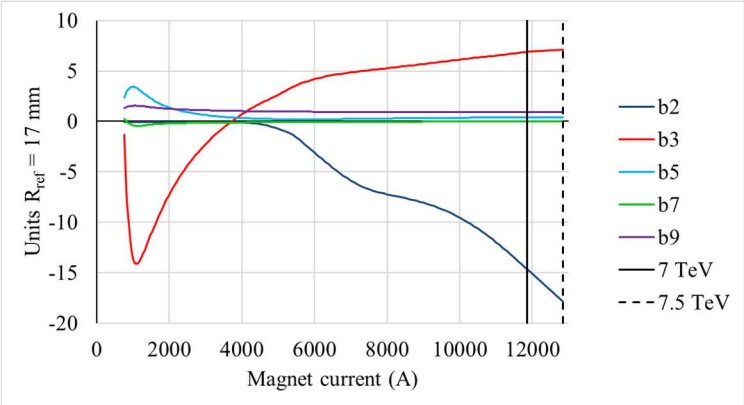

Figure 5: Field errors as a function of the magnet current from injection to top energy, in units of 10^{-4} the main field at a reference radius of 17 mm.

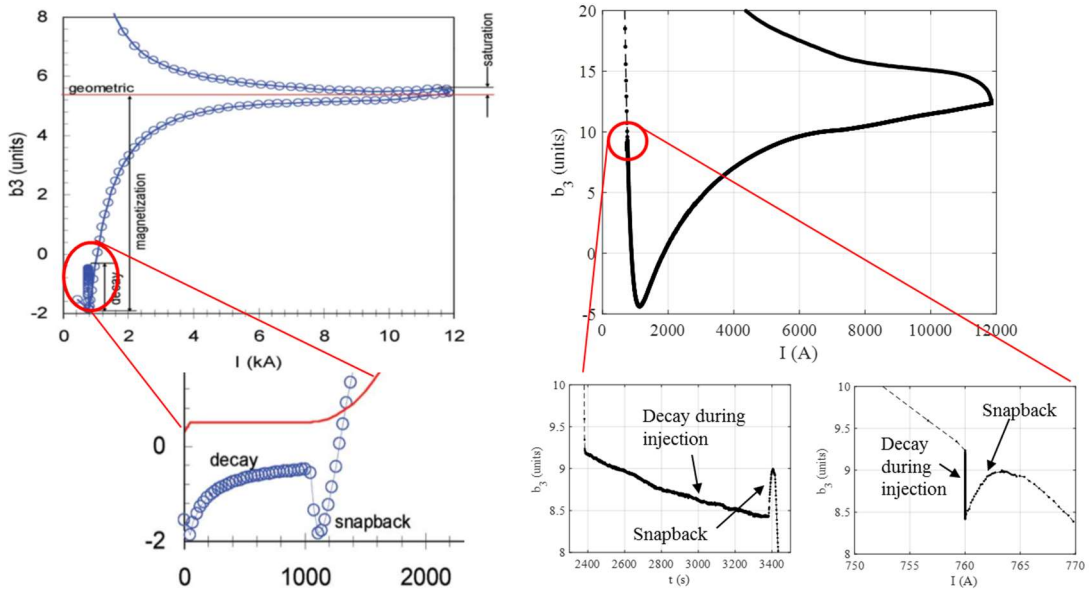

Figure 6: Typical decay and snapback for an LHC Machine Cycle for the LHC-MB dipole (left) and for the 11 T dipole (right).

At low energy, multipole errors are dominated by the persistent currents in the superconductor. Due to the large filament size of the superconducting elements (effective filament size around 10 times larger than in the Nb-Ti LHC MB Dipoles) and higher current density, persistent current effects in the 11 T magnets are almost 3 times larger than in the nominal MB. The beam is injected at an energy level lower than the penetration field of the superconductor. The maximum contribution to the sextupole component is -21 units at 1.1 kA. Figure 5 shows the allowed field errors as a function of the magnet current level including geometric, persistent currents and iron saturation effects.

Dynamic defects in the superconductor are also different in Nb_3Sn and Nb-Ti. For the dipole, the decay of the sextupole gives a large chromaticity change during injection and ramp if it is not controlled properly. The present understanding of the decay is that the local field changes due to current redistribution during a constant current plateau cause a decrease of the average filament magnetization. In the case of the 11 T dipoles, the changes on b_3 and b_5 during a standard operation cycle at 1.9 K appear as a net increase of the average filament magnetization. As soon as the field is ramped up again after the end of injection, the magnetization rapidly recovers and in most of the cases follows the original hysteresis curve. This snap-back is about four times faster than the one observed in LHC-MB dipoles [8]. Figure 6 compares the typical decay and snapback in a LHC-MB dipole and in an 11 T dipole.

At top energy the field errors are comparable to those of the nominal LHC MB dipole magnets, except for the b_3 sextupole component which is of the same sign but approximately 3 times larger as in the nominal LHC MBs causing challenges for the b3 correction at top energy (see below in Section 3.3).

Implementing new correction procedures and algorithms will require extensive magnet measurements and modelling and commissioning time. The LHC correction procedures have been evolved much over the first Run of the LHC operation and the Run 2 operation has largely benefited from the developments and measurements during the first three years of LHC operation. Recommissioning the new magnet and correction system after the installation of the new 11 T dipole magnets will therefore require time and dedicated machine studies.

3.3 Strength limitations of existing HL-LHC magnets that exclude operation beyond 'ultimate' beam energy

In section 3.2.4 it has already been mentioned that all superconducting separation dipoles should be replaced to cope with the increased beam energy. Moreover, the triplet magnets will most likely have to be replaced, too, both the new ones developed for HL-LHC and those from the LHC time still installed in IR2 and 8 as all of them have been only specified up to 'ultimate' beam energy.

As far as the other insertion magnets are concerned, we give in the following a list of limiting devices for two possible beam energies. Both round and flat optics for HL-LHC V1.3 have been considered. It is worth noting that the required gradients have been increased by 1% to consider some extra strength needed for the optics corrections. The following magnet circuits have been identified to require setting that are beyond the magnet specifications:

- Beam energy of 7.75TeV: Q5.R4, Q5.L6, Q5.R6, Q6.R4, Q7.L1, Q7.R1, Q7.R4, Q7.L5, Q7.R5, Q8.L2, Q8.L4, Q8.R4, Q8.L6;
- Beam energy 8.08TeV: Q5.R4, Q5.L6, Q5.R6, Q6.R4, Q7.L1, Q7.R1, Q7.L2, Q7.R4, Q7.L5, Q7.R5, Q7.L8, Q7.R8, Q8.L2, Q8.L4, Q8.R4, Q8.L6, Q8R6, Q8.R8, QTL9.L7, Q10.L6, QT12.L6, QT13.R4;

Figure 7 shows the required relative strength beyond 'ultimate' for the two possible beam energies, including the information about which optics is generating the extra strength.

For the main quadrupole circuits, we assume that one can devise an optics configuration in which they can be used in their existing powering configuration.

The situation in terms of strength for the correctors' circuits is not critical, apart from lattice sextupoles and spool pieces and that situation will be discussed next.

The correction circuits of the LHC rings deserve a more detailed consideration. While the circuits different from the lattice sextupoles seem to have a reasonable margin, based on their usage during Run 2 operations, the lattice sextupoles in the strong ATS arcs are already very close to their limits. This means that any energy increase of the LHC will be difficult in terms of chromaticity control at top energy. A possible mitigation could be the use of a 60 degree lattice [10]. However, studies on this topic are still ongoing and the full implications of such a solution still need to be evaluated.

A similar situation occurs for the sextupolar spool pieces, whose performance is not suitable for the proposed upgrade. This is linked, mainly to the field quality of the 11 T dipole at top energy. In fact, the large systematic sextupolar component (see Table 4, note that to compare the field quality of the 11 T dipoles with that of the well-known main magnets an appropriate rescaling by the magnetic field should be applied) at high field creates a very large imbalance between the b_3 in the Ni-Ti dipoles and that of the Nb_3Sn dipoles. The sextupolar spool pieces can cope with the correction of about 4 units (of Nb-Ti magnets) at 7.75 TeV and 3.9 units at 8.08 TeV. Therefore, a large uncompensated b3 component will be present in both rings. Note, also, that the increased values of the beta-function in the arcs due to the ATS optics will further enhance the chromatic effects induced by the uncompensated b_3 component. A rough estimate of the impact on linear chromaticity of such an uncompensated b_3 component gives about 70 and 50 units of chromaticity in the horizontal and vertical planes, respectively. This occurs for the nominal HL-LHC optics with round beta* of 15 cm. Clearly, such a large chromaticity is not desirable as, in addition to the perturbation of the linear optics, it might have an impact on the beam lifetime. Albeit some studies at the LHC have shown that a large systematic b3 does not necessarily impact on the beam lifetime, such a configuration is certainly non-ideal form the operation point of view [10]. Higher-order effects have not been evaluated in detail, but the strong perturbation of the linear optics already indicates that non-linear effects will induce a strong perturbation of the beam dynamics.

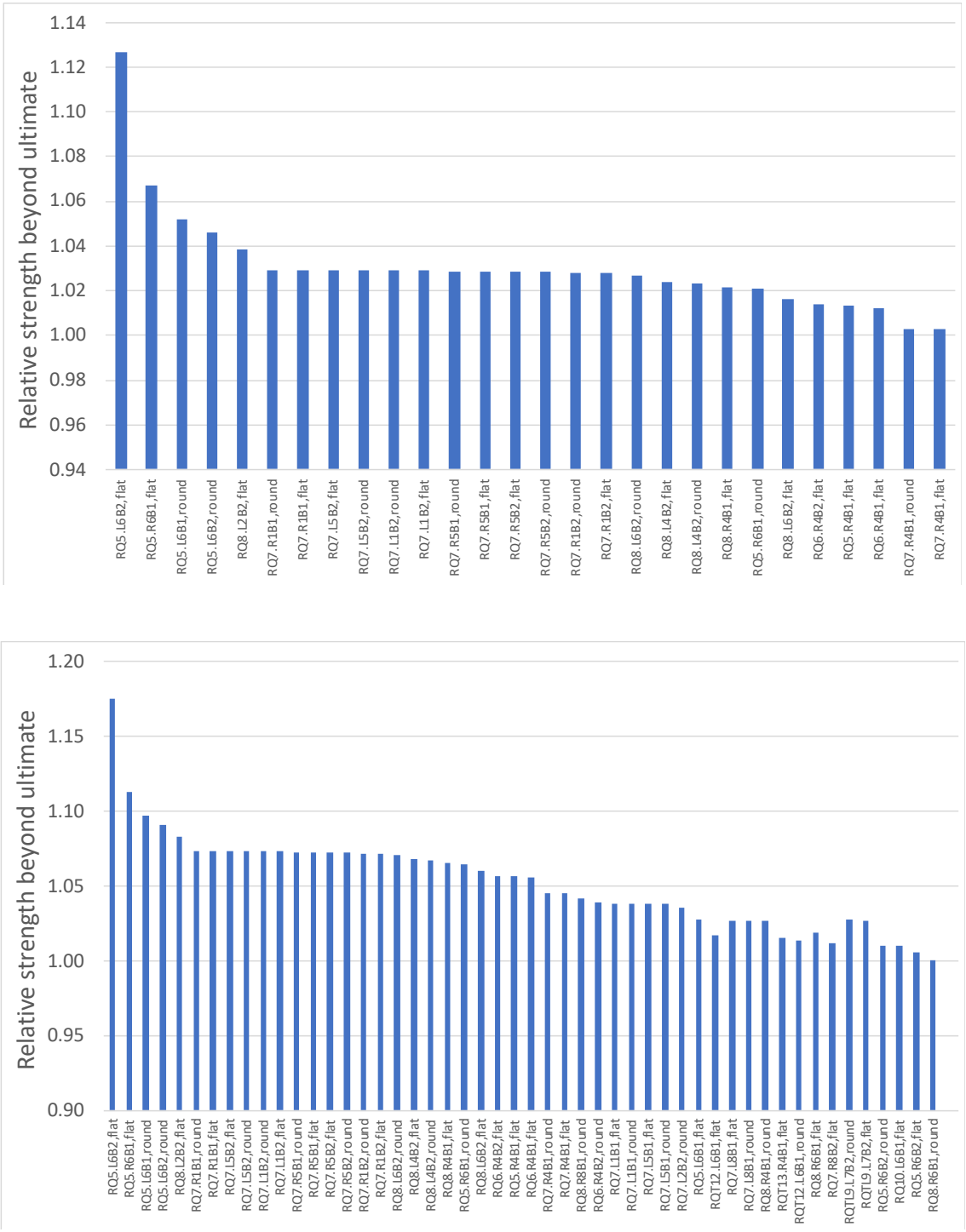

Figure 7: List of quadrupoles running beyond ultimate energy for a beam energy of 7.75 TeV (upper) or 8.08 TeV (lower). The information about which optics is generating the strength issue is also shown.

At injection energy, the main issue is the control of the dynamic effects. In fact, as already mentioned, the snapback effect of the Nb-Ti and Nb_3Sn magnets is of different sign and amplitudes (see Figure 6), which increases the difficulty to control the impact on the beam dynamics at the beginning of the energy ramp. For the HL-LHC 11 T Nb_3Sn installation in the dispersion suppressors, the operation can rely on dedicated individually powered dipole corrector magnets to cope with that. A replacement of $1/3^{rd}$ of the arc dipole magnets one cannot rely on such a setup.

It is also worth mentioning that the field quality of the 11 T dipoles will enhance any feed-down effect from orbit. In particular, the large b_3 component will generate non-negligible beta-beating, in case of horizontal orbit errors, or coupling, in case of vertical orbit errors. Consider also, that the ATS optics comes with voluntary orbit bumps used to compensate dispersion effect: these would probably no longer be feasible due to the side effects induced by feed-down.

3.5 Beam Dump System related aspects

The studies in the second report on the LHC full energy exploitation underlined that the LHC Beam Dump System (BDS) needs to be already upgraded for operation at 'ultimate' beam energy. Pushing the operational beam energy beyond this value will only strengthen this point. In case the decision on a higher than 'ultimate' beam energy is taken sufficiently early, the increased beam energy can probably be incorporated in the planned BDS upgrades, e.g. new beam dump core and mechanical design and dump window designs. However, for the BDS upgrades already planned for LS2, e.g. capacitor and high voltage system upgrade for the BDS, this request will come too late and implies most probably additional upgrades for the LHC BDS.

3.6 Machine Protection related aspects

The changes in the magnet powering system will required considerable changes to the current LHC magnet protection infrastructure, notably an upgrade of the individual magnet protection system. While a solution using 16 quench heater power supplies has been already studied and developed for the 5m long straight 11 T magnet design in the context of the HL-LHC project, the protection of a single 15m long Nb_3Sn magnet will represent a considerable challenge, most likely requiring in addition to the multiplication of quench heaters the deployment of CLIQ units for each 11 T unit. Additional changes will be required to adapt the so-called nQPS layer, and the increased stored energy in the circuit will require changes and upgrades to the 13 kA EE systems.

The increase in beam energy will further reduce the operational margins but is not expected to reveal additional show-stoppers but rather to translate in the loss of machine efficiency and availability when compared to operation at ultimate energy of 7.5 TeV. Similar upgrades of extending the controls and operational ranges beyond ultimate energy (as already outlined for the energy tracking systems and BDS) will however become necessary for additional systems such as beam instrumentation (BLMs) and collimation.

4 Machine Efficiency and Availability

For operation at 8.08 TeV, most of the considerations made in the report on LHC ultimate energy are still applicable. In particular, the higher energy stored in the beams and in the magnets implies even longer quench recoveries. Based on experience from the 2016 training campaign, quench recovery times of more than 13 hours can be expected when going from 6.5 to 8.08 TeV operation. This estimate highly depends on the number of secondary quenches. Furthermore, when increasing the beam energy, the magnet quench levels will decrease. This, combined with an increase of energy deposition in the coils per lost proton, leads to an increase in the number of UFO induced beam aborts (even for constant number of UFOs in the beam vacuum system) which could completely jeopardize LHC operation, especially in early phases of operation following a long shutdown. Better insights on the deconditioning

effects following long shutdowns with respect to UFO rates will be available at the beginning of LHC Run 3.

Concerning magnet performance, the remaining LHC dipoles will be pushed to the extreme in this scenario, with very small operational margins for e.g. UFO losses or cryogenic instabilities.

Shorts-to-ground and inter-turn shorts (as observed already during magnet during training campaigns, standard beam operation and while testing in SM18) are considered more likely to appear given the higher field and stored energy associated to operation at 8.08 TeV. Another factor that should be considered is the potentially faster degradation of quench heaters due to the possible higher number of discharges following quenches. An assessment of the long-term performance of quench heaters for Nb_3Sn magnets will only be possible after LS2.

All power converters were already tested above ultimate parameters (notably at their so-called rated power), including the related power converter infrastructure (but not e.g. the normal-conducting or water-cooled cables). Based on these elements, no major impact on the power converter failure rate is expected when further increasing the beam energy, thanks to available margins.

The LBDS is expected to be particularly affected by the energy increase, even considering the upgrades deployed in LS2, as the system was not conceived to reach beyond-ultimate parameters. Several asynchronous dumps per year could be expected running at 8.08 TeV, unless major upgrades are envisaged.

As stated in section 3.1, the LHC cycle duration is expected to increase due to the performance limitations of the cryogenic system, which will be operated without any margins. An average increase of the turnaround of 1 hour is therefore to be expected (including also the increase of the time for magnet ramps).

Two scenarios were defined to account for the effects discussed above. An optimistic scenario, were the only performance loss comes from the additional turnaround time with respect to 7.5 TeV operation due to the cryogenic system. A conservative scenario, in which in addition all factors described above contribute to increased failure rates and repair times of the machine.

5 Potential Performance Reach

We assume that the main operational parameters for the LHC operation beyond 7.5 TeV (minimum β*, crossing angle, etc.) are the same as at 7 TeV, except for the average turnaround time, which was assumed to be 5 h for the case of operation at ultimate beam energy (7.5 TeV) and to which we added one hour in this report in order to account for the additional cryo cooling time due to the magnetic hysteresis heating of the 11 T dipole magnets: 6 hour average Turnaround time for operation 'beyond the ultimate energy' case. If keeping the same main operational parameters is even feasible with the existing HL-LHC Insertion Regions is currently not guaranteed. A possible reduction in β^* reach might be implied by the limited magnet strength of the existing IRs. But without following up on this detail, the performance reach is expected to decrease even for the same optics configuration due to the increase cycle time and the reduced operation margins for the magnet and cryogenic systems.

Table 5 summarizes the expected performance losses for operation at nominal, ultimate and beyond ultimate beam energy for the ‘conservative’ and ‘relaxed’ assumptions. In the conservative scenario the starting point are the 2016 fault distributions for all systems, as 2016 was affected by isolated long stops, which have not been observed in 2017. For the relaxed scenario, the 2017 fault distributions are taken instead as reference [2]. In addition to these basic fault distributions, failures specifically associated to the respective beam energy operation are considered. While the HL-LHC performance goal of 250 fb^{-1} per year is still within reach for the ‘Relaxed’ fault assumptions, the luminosity loss is up to 40 % comparing operation at 7 and 8.08 TeV (7 TeV ‘conservative’ and 8.08 TeV ‘conservative’).

Table 5: Expected performance reach for operation at nominal, 'ultimate' and 11 T boosted beam energies for the 'conservative' and 'relaxed' operation and fault assumptions.

	7 TeV		7.5 TeV		8.08 TeV	
	Conservative	Relaxed	Conservative	Relaxed	Conservative	Relaxed
Availability [%]	67	74	50	71	45	71[2]
Integrated Luminosity [fb^{-1}]	278	297	188	282	165	268

Given the statement by the experiments in the second report on the LHC full energy exploitations that the total loss in integrated luminosity should be less than 20% when compared to a continuous operation at nominal beam energy, the studied scenario does not appear to be very attractive for the experiments.

6 Summary and Conclusion

Given the already marginal gain in beam energy, 8.08 TeV even for the most optimistic scenario with 14.5 m long 11 T dipole magnets compared to the 'ultimate' beam energy of 7.5 TeV, i.e. at most a 7.7% increase, the rather long lead time for the magnet adaptation to the LHC arc cell, estimated at at least 10 years, the disadvantageous consequences from the HL-LHC 11 T cable design, e.g. magnetic induction heating during the magnet cycle and less than optimum field quality, and the fact that several of the LHC magnet circuits will ran out of strength for beam energies above 'ultimate', the proposal of replacing 1/3rd of the nominal Nb-Ti magnets with Nb_3Sn 11 T dipole magnets from the HL-LHC upgrade appears as a rather unattractive and costly upgrade. Even the 'lowest cost' estimate for replacing one third of the arc dipole magnets by 11 T magnet amounts to over 3 BCHF based on the HL-LHC 11 T magnet design, and that is without considering any other upgrades in the machine like, for example, magnets in the dispersion suppressor sections and the dogleg and separation-recombination dipole magnets in the long insertions, or other systems like the beam dump or the magnet circuits. The electrical characteristics of the circuit will be very different, with discontinuities at every magnet. This will probably change dramatically the transient response of the circuit, affecting powering, detection, Electro-Magnetic-Coupling in case of quench or dump, requiring most likely substantial upgrades in the LHC circuits and QPS systems.

This becomes even more pronounced if one considers that the exploitation can, at best, be conducted over one 3 year running period, due to the lifetime limit of HL-LHC components. Adding to this consideration the expected loss in integrated luminosity of up to 40 % (comparing operation at 7 TeV 'conservative and 8.08 TeV 'conservative' with reduced margins and increased cycle times and the time necessary for recommissioning the optics and non-linear correction systems) and considering the significant cost for such a supposedly 'Quick & Easy' upgrade, it appears far more attractive to pursue an energy upgrade of the LHC beyond the 'ultimate' beam energy in the framework of a proper HE-LHC design, together with a complete re-optimization of the magnets and cables (field quality, cost and magnetic induction heating), vacuum (electron-cloud and beam screen design in the presence of synchrotron radiation) and cryogenic systems (optimum operational temperature for Nb_3Sn magnets) and dispersion suppressor and interaction region layout. Such an approach promises a far higher energy reach and a much better cost / performance ratio (increased beam energy and possible operation time per spent MCHF)!

[2] The increase in turnaround time due to the required cryogenic recovery time does not change the machine availability as it is not connected to a technical fault

7 References

[1] O. Brüning *et al.*, 'LHC Full Energy Exploitation Study: Operation at 7 TeV', CERN-ACC-2017-0086.

[2] O. Brüning *et al.*, 'LHC Full Energy Exploitation Study: Operation at Ultimate Energy of 7.5 TeV', CERN-ACC-2019-0015.

[3] R. Bruce, C. Bracco, R. De Maria, M. Giovannozzi, S. Redaelli, R. Tomas Garcia, F.M. Velotti, J. Wenninger, Parameters for aperture calculations at injection for HL-LHC, CERN-ACC-2016-0328.

[4] R. Bruce, C. Bracco, R. De Maria, M. Giovannozzi, S. Redaelli, R. Tomas Garcia, F.M. Velotti, J. Wenninger, Updated parameters for HL-LHC aperture calculations for proton beams, CERN-ACC-2017-0051.

[5] S. Fartoukh, M. Giovannozzi, D. Missiaen, E. Todesco, F. Zimmermann, Considerations on a Partial Energy Upgrade of the LHC, ARIES-2017-001; CERN-ACC-2017-096.

[6] http://lhc-optics.web.cern.ch/lhc-optics/www/hllhc13/

[7] https://lhc-div-mms.web.cern.ch/lhc-div-mms/tests/MAG/docum/hilumi/Magnets/field_quality.xlsx

[8] S. Izquierdo Bermudez, L. Bottura, L. Fiscarelli, E. Todesco, Decay and Snapback in Nb3Sn Dipole Magnets, IEEE Transactions on Applied Superconductivity, Year: 2017, Volume: 27, Article Sequence Number: 4002306.

[9] M. Hofer, "Experience with strong uncorrected sextupolar errors in the LHC dipoles", ABP Group Information Meeting, 18 July 2019, https://indico.cern.ch/event/834321/

[10] Jaqueline Keintzel, "A 60 degree arc cell LHC lattice for energy upgrades", Optics Measurement and Correction meeting, 10 Sep 2019, https://indico.cern.ch/event/846683/

[11] J. Keintzel J. Keintzel, R. Tomás, R. Bruce, M. Giovannozzi, T. Risselada, F. Zimmermann, "Lattice and optics options for possible energy upgrades of the Large Hadron Collider", Submitted for publication in Phys. Rev. Accel. Beams.